# Characterization by Dynamic Indentation on Laser-Treated WC-Ti Coatings Deposited via Cold Gas Spray

Lidia Baiamonte*, Laura Paglia, Virgilio Genova, Marco Conti, Giulia Pedrizzetti, Cecilia Bartuli

Dept. of Chemical Engineering Materials Environment, Sapienza University of Rome – INSTM Reference Laboratory for Engineering of Surface Treatments, Via Eudossiana 18, 00184 Rome, RM, Italy
lidia.baiamonte@uniroma1.it

The present work is focused on the characterization of WC-Ti coatings via dynamic indentation, by which the elastic modulus and hardness were evaluated.The coatings were obtained by Cold Gas Spray (CGS) and then post-treated with a diode laser, to promote the in-situ formation of TiC through a controlled decarburization of the WC phase and the following reaction with the metallic Ti. WC-Ti is, in fact, a promising composition for wear applications due to the high content of carbides following the heat treatment, and to the presence of Ti as the metallic binder as a suitable alternative to the more common cobalt. The characterization of the WC-Ti coatings is thus necessary to verify their suitability as a possible alternative to other hardmetal formulations, such as WC-Co-based thermal sprayed coatings.Dynamic indentations were performed on the as-sprayed as well as on the laser-treated coatings. The laser power-scan rate scenarios used in this study were 250 W-8 mm/s and 350W-8 mm/s.Two loads, 500 mN and 1000 mN, were applied. The resulting load/penetration curves were then elaborated using the Oliver-Pharr theory for dynamic indentations, by which the Young's modulus and the hardness were finally calculated. Results showed an increase in the elastic modulus of the laser-treated samples, with the highest values – around 300 GPa, versus the 195 GPa evaluated on the as-sprayed sample - registered for the sample treated with the 350W- 8 mm/s set of parameters.

## 1. Introduction

Ceramic-metallic hardmetal coatings, also referred to by their abbreviated form as *cermets*, are a popular class of materials widely used in applications where tribological and corrosion resistance are required. WC-Co-based coatings, generally produced via thermal spray routes, especially via high velocity oxygen-fuel (HVOF), are the most used wear-resistant cermets, due to their outstanding properties (Baiamonte et al., 2014; Mateen et al., 2011; Picas et al., 2009); however, the current research on hardmetal coatings is focusing on finding a suitable alternative to cobalt as metallic binder, because of its relatively recent classification as Critical Raw Material (Tkaczyk et al., 2018).

A previous study by Tang et al., 2018 explored the possibility of replacing cobalt with titanium as metallic matrix: specifically, in their study WC-Ti reactive powders were deposited via Cold Gas Spray process, and the resulting layers subsequently underwent a furnace heat-treatment to aid the formation of the hard TiC phase by the effect of a Self-propagating High-temperature Synthesis (SHS) reaction (Levashov et al., 2017). In a more recent study (Baiamonte et al., 2021), the feasibility of laser post-treatment in comparison to the furnace heat-treatment was assessed, finding that the irradiation of the surface with a low-to-medium power laser beam successfully triggered the SHS reaction, increasing the Vickers microhardness of the treated material and improving its tribological performance. In the attempt to deepen the understanding of the mechanical properties of the laser-treated WC-Ti coatings, the present investigation aims to evaluate elastic modulus and hardness from a microscopic perspective by mean of dynamic indentation. Two loads, 500 and 1000 mN, were applied on the surfaces that were laser-treated with two different power levels, and the results were then compared to those collected for the as-sprayed coating.

## 2. Materials and methods

The samples were prepared by depositing high energy ball milled WC50Ti powders (produced by MBN Nanomaterialia, Treviso, Italy) via Cold Gas Spray onto steel substrates. Laser post-treatment was performed using a Rofin Sinar DL015 diode laser, with an elliptical spot size of 3.8 x 1.2 mm and a characteristic wavelength of 940 mm. Two sets of parameters were selected for laser-treatment: 250 W power and 8 mm/s scan rate, and 350 W and 8 mm/s scan rate. The samples used in the present study are resumed in Table 1:

*Table 1: samples and nomenclature*

| Sample ID | Laser power [W] | Scan rate [mm/s] |
|---|---|---|
| AS | - | - |
| L1 | 250 | 8 |
| L2 | 350 | 8 |

Further details on the deposition process and optimization of the power-scan rate combinations can be found in the previous work of Baiamonte et al., 2021.

Dynamic indentation was carried out on the as-sprayed as well as on the laser-radiated samples, to evaluate elastic modulus and hardness according to ISO 14577-4:2007 standard. A Nanotest (MicroMaterials Ltd., Wrexham, UK) instrumented indentation equipment was used; two maximum loads, 500 and 1000 mN, were applied for 10 s through a 3-sided Berkovich indenter, with a loading-unloading rate of 50 mN/s (Marra et al., 2016). The load values were carefully chosen to minimize the volume being measured, ensuring that only the laser treated layer would be evaluated, and increasing the likelihood of measuring a defect-free zone. The load/penetration curves were analyzed using Oliver and Pharr's approach(Oliver & Pharr, 2004). The reduced elastic modulus was calculated using Eq. (1):

$$E_r = \frac{1}{2}\sqrt{\frac{\pi}{A}}\frac{dp}{dh} \tag{1}$$

in which A is the area of the indenter, and dp/dh is the elastic contact stiffness, that is, the slope of the unloading curve at the maximum load. The Young's modulus was then extracted from Eq. (2):

$$\frac{1}{E_r} = \left(\frac{1-v_s^2}{E_s} + \frac{1-v_i^2}{E_i}\right)^{-1} \tag{2}$$

using the reduced elastic modulus calculated in Eq. (1). $E_s$, $E_i$, $v_s$ and $v_i$ are the Young's moduli and the Poisson ratios of specimen and indenter, respectively. A Poisson ratio of 0.28 was assumed in the calculations. A total amount of 30 indentations per load were performed on each surface.

## 3. Results and Discussion

Both the reduced elastic moduli and hardness values were converted into elastic moduli as per Eq. (2), and Vickers hardness. Young's moduli, as shown in Figure 1, increases with increasing laser power. The value of the elastic modulus calculated at the lower load is generally higher because of the area of the indenter, as reported in Eq. (1).

However, the modulus evaluated at 1000 mN (301.45 GPa) on the L2 sample results to be higher than the one calculated at 500 mN (283.03 GPa). A possible explanation for such result lies on the phase composition of the L2 sample, as reported in the previous study on WC-Ti coatings: the laser heat-treatment brought to the formation of the hard TiC phase and of the solid solution of W and Ti that, together with the already existing hard WC particles, contributed to the dramatic increase in microhardness. This means that, in the L2 sample, the co-existence of two different hard reinforcement embedded in the remaining Ti matrix may result in a bimodal composition that directly affects the elastic modulus of the material.
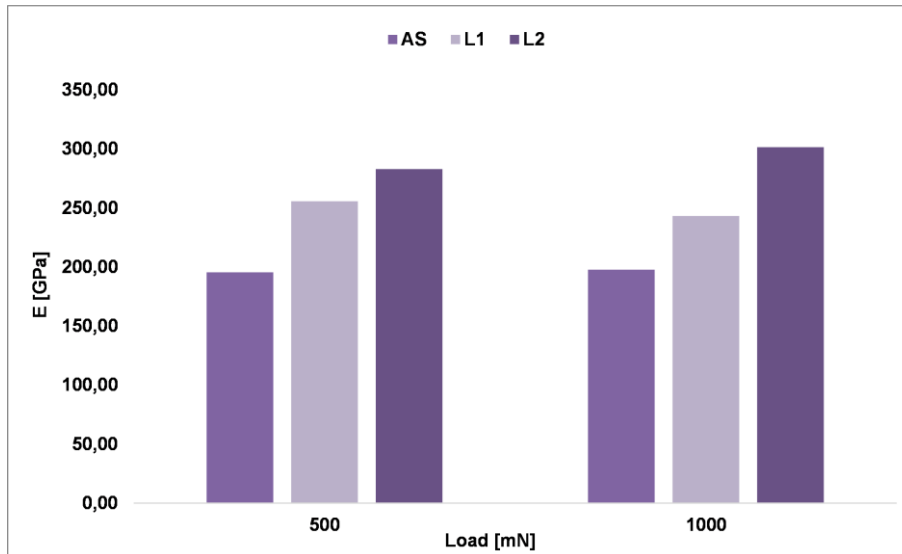
*Figure 1: comparison of the Young's modulus calculated with 500 and 1000 mN loads on the AS, L1 and L2 WC-Ti coatings.*

In Figure 4, representative load-unload curves for each sample and load are shown. The depth penetration tends to progressively decrease going from the AS to the L2 sample, as the laser treatment has changed the microstructure of the WC-Ti cermet by increasing its microhardness. The slopes of both the 500 and the 1000 mN mean curves are the same in the AS sample; the same behavior can be observed in the L1 mean curves. It can be inferred that the laser post-treatment in the L1 coating leads to a change in the microstructure that is overall homogenous. On the other hand, curves from the L2 sample exhibit two different classes of slopes: such result could be ascribed to the aforementioned bimodal structure, in which the TiC formed following the 350 W laser treatment coexists with the hard WC phase and the solid solution of W and Ti. Thus, the double reinforcement may have led to a double class of slopes in the load-unload curves, depending on the zone penetrated by the Berkovich indenter.
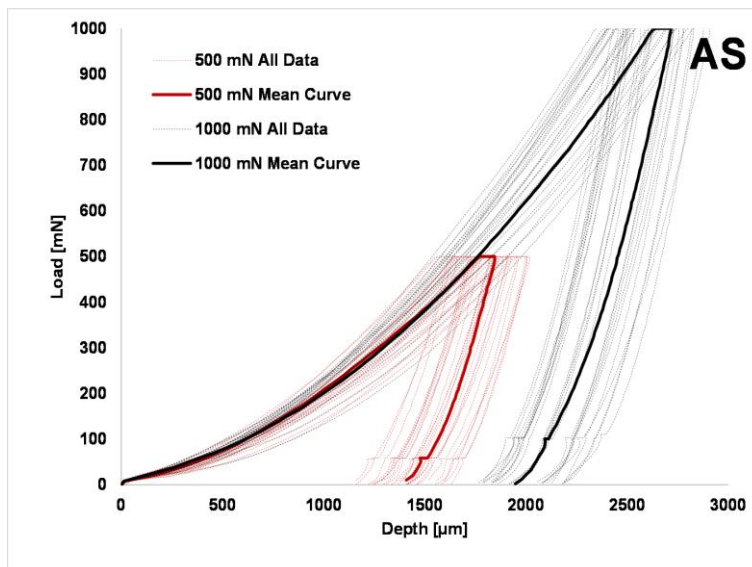


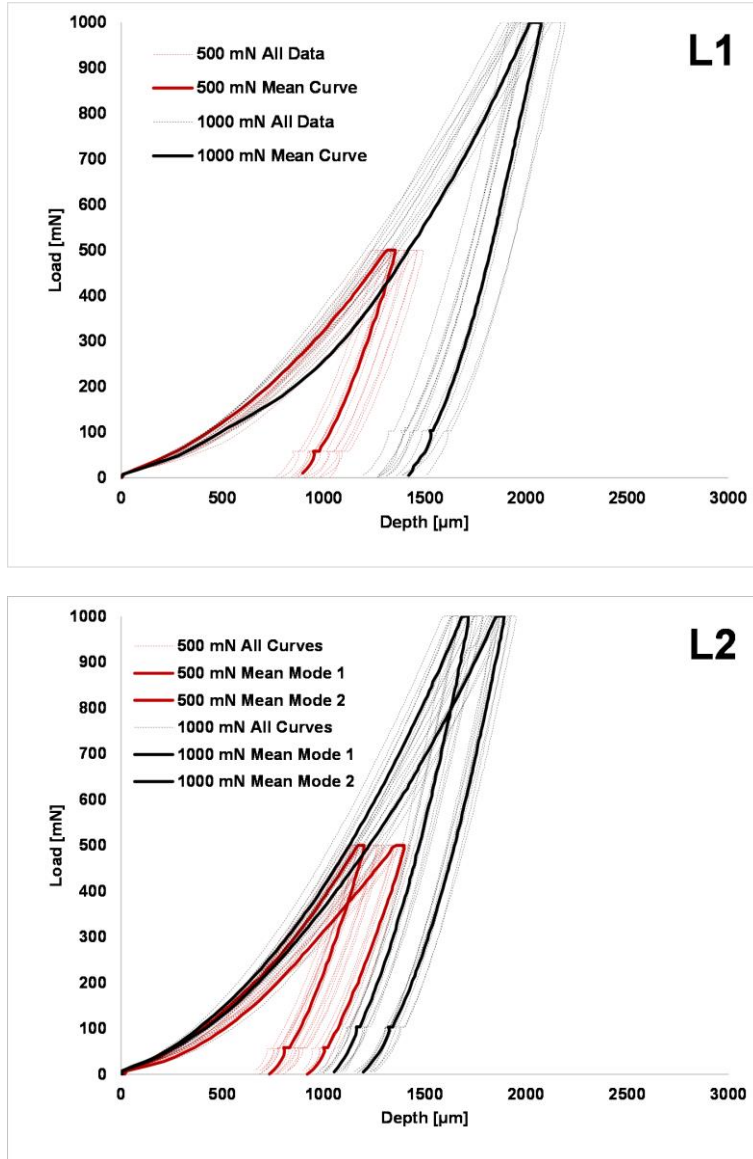*Figure 2: load-unload curves of the AS, L1 and L2 WC-Ti samples.(continue)*

*Figure 3: load-unload curves of the AS, L1 and L2 WC-Ti samples.*

As for the Vickers hardness (Figure 4), it increases with increasing laser power; for each sample, values of hardness evaluated at the 500 mN load are only slightly higher than those calculated with the 1000 mN load. Such results are consistent with the microhardness analysis carried out in the previous study by Baiamonte et al., 2021, where the Vickers microhardness would dramatically increase with increasing laser power, that resulted in the formation of the hard TiC phase. However, values calculated by means of the instrumented indentation expectedly result higher than the corresponding ones evaluated through Vickers indenter, because of the different areas involved in both analysis. It is important to emphasize that data resulting from the instrumented indentation analysis are evaluated on a microscopic scale and are hence different from the corresponding mechanical properties calculated with other characterization techniques.

There are no data in literature reporting Young's modulus and hardness for cold-sprayed WC-Ti coatings; however, when comparing the obtained values to those of simple cold-sprayed Ti6Al4V coatings as in the study of Garrido et al., 2018, those calculated in the present investigation are expectedly higher because of the presence of WC particles.
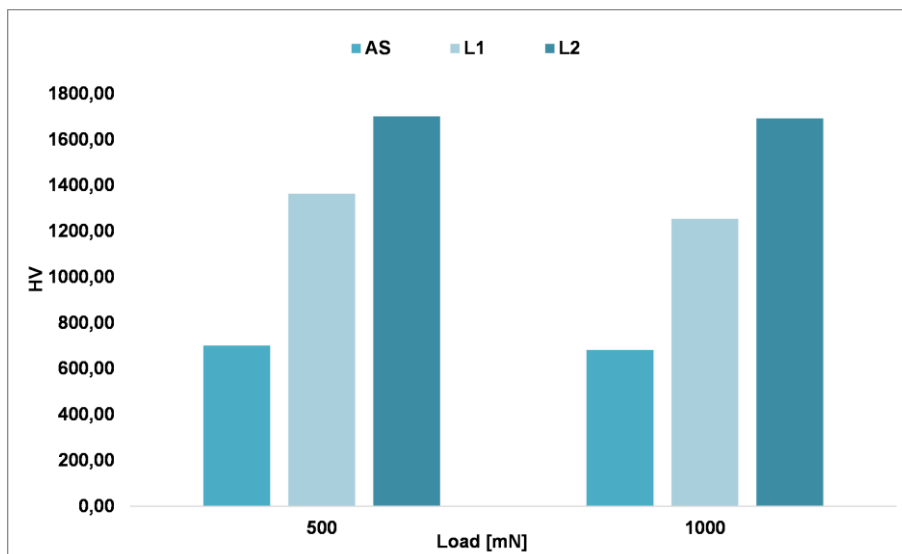
*Figure 4: comparison of the Vickers microhardness calculated with 500 and 1000 mN loads on the AS, L1 and L2 WC-Ti coatings.*

## 4. Conclusions

A mechanical characterization of cold-sprayed WC-Ti coatings, both as-sprayed and post-treated with a laser beam, was carried out from a microscopic perspective. The elastic modulus and microhardness were evaluated by means of instrumented indentation.

The analysis yielded the following results:

1. The Young modulus increases with the intensity of the heat treatment, due to the formation of TiC. However, a bimodal behavior has been observed in the L2 sample, probably due to the presence of different hard phases with different properties. This supposedly bimodal behavior is particularly emphasized in the load-unload curves, in which two different slopes of the mean curves per load can be observed.
2. The hardness increases with the power of the laser treatment, again due to the formation of the hard TiC phase. This result was expected according to the experimentation carried out in the previous study by Baiamonte et al., 2021, and confirms that an increase in hardness occurs also on a microscopic scale.

While further studies are needed to better understand the properties of WC-Ti cold-sprayed coatings, the results gathered so far are encouraging in the attempt to design new Co-free formulations for wear-resistant cermet materials. Such characterization is a further step towards comprehending WC-Ti coatings obtained from reactive powders, providing a deeper insight into their properties. A direct comparison with more common compositions, such as WC-Co-based materials, will be necessary for future investigations.

**Reference**

Baiamonte, L., Pulci, G., Gisario, A., Paglia, L., Marino, A. L., Tului, M., & Marra, F. (2021). WC-Ti Coatings Deposited Via Cold Gas Spray and Modified by Laser and Furnace Heat Treatments. *Journal of Thermal Spray Technology*, *30*(8), 2083–2098. https://doi.org/10.1007/s11666-021-01278-9

Baiamonte, L., Pulci, G., Hlede, E., Marra, F., & Bartuli, C. (2014). Thermal spray coatings for corrosion and wear protection of naval Diesel engines components. *Metallurgia Italiana*, *106*(6), 9–13.

Garrido, M. A., Sirvent, P., & Poza, P. (2018). Evaluation of mechanical properties of Ti6Al4V cold sprayed coatings*. *Surface Engineering*, *34*(5), 399–406. https://doi.org/10.1080/02670844.2017.1398442

*ISO - ISO 14577-4:2007 - Metallic materials — Instrumented indentation test for hardness and materials parameters — Part 4: Test method for metallic and non-metallic coatings*. (n.d.). Retrieved February 14, 2023, from https://www.iso.org/standard/39228.html

Levashov, E. A., Mukasyan, A. S., Rogachev, A. S., & Shtansky, D. v. (2017). Self-propagating high-temperature synthesis of advanced materials and coatings. *International Materials Reviews*, *62*(4), 203–239. https://doi.org/10.1080/09506608.2016.1243291

Marra, F., Baiamonte, L., Bartuli, C., Valente, M., Valente, T., & Pulci, G. (2016). Tribological behaviour of alumina-titania nanostructured coatings produced by air plasma spray technique. *Chemical Engineering Transactions*, *47*, 127–132. https://doi.org/10.3303/CET1647022

Mateen, A., Saha, G. C., Khan, T. I., & Khalid, F. A. (2011). Tribological behaviour of HVOF sprayed near-nanostructured and microstructured WC-17wt.%Co coatings. *Surface and Coatings Technology*, *206*(6), 1077–1084. https://doi.org/10.1016/J.SURFCOAT.2011.07.075

Oliver, W. C., & Pharr, G. M. (2004). Measurement of hardness and elastic modulus by instrumented indentation: Advances in understanding and refinements to methodology. *Journal of Materials Research*, *19*, 3–20. https://doi.org/doi.org/10.1557/jmr.2004.19.1.3

Picas, J. A., Xiong, Y., Punset, M., Ajdelsztajn, L., Forn, A., & Schoenung, J. M. (2009). Microstructure and wear resistance of WC–Co by three consolidation processing techniques. *International Journal of Refractory Metals and Hard Materials*, *27*(2), 344–349. https://doi.org/https://doi.org/10.1016/j.ijrmhm.2008.07.002

Tang, J., Saha, G. C., Richter, P., Kondas, J., Colella, A., & Matteazzi, P. (2018). Effects of Post-spray Heat Treatment on Hardness and Wear Properties of Ti-WC High-Pressure Cold Spray Coatings. *Journal of Thermal Spray Technology*, *27*, 1153–1164. https://doi.org/10.1007/s11666-018-0762-7

Tkaczyk, A. H., Bartl, A., Amato, A., Lapkovskis, V., & Petranikova, M. (2018). Sustainability evaluation of essential critical raw materials: Cobalt, niobium, tungsten and rare earth elements. *Journal of Physics D: Applied Physics*, *51*(20), 203001. https://doi.org/10.1088/1361-6463/aaba99